Dielectric, piezoelectric, and elastic properties of the Rochelle salt $NaKC_4H_4O_6 \cdot 4H_2O$: A theory

R. R. Levitskii,[1] I. R. Zachek,[2] T. M. Verkholyak,[1] and A. P. Moina[1]
[1]*Institute for Condensed Matter Physics, 1 Svientsitskii Street, Lviv, UA-79011, Ukraine*
[2]*National University "Lvivs'ka Politekhnika," 12 Bandera Str., Lviv, UA-79013, Ukraine*
(Received 20 June 2002; revised manuscript received 18 November 2002; published 28 May 2003)

We modify the conventional Mitsui model by including the terms related to piezoelectric coupling with shear strain ε_4. The static and dynamic dielectric, piezoelectric, and elastic characteristics of a Rochelle salt crystal are calculated. It is shown that taking into account piezoelectric effects yields a correct temperature behavior of the relaxation times and the dynamic dielectric permittivity of the Rochelle salt in the vicinity of the transition points.

DOI: 10.1103/PhysRevB.67.174112 PACS number(s): 77.65.Bn, 77.22.Gm, 77.80.Bh

I. INTRODUCTION

It is generally accepted that the Rochelle salt (double sodium-potassium tartrate $NaKC_4H_4O_6 \cdot 4H_2O$) has two Curie points. The ferroelectric phase exists in a rather narrow temperature interval from $T_{C1}=255$ K to $T_{C2}=297$ K. Spontaneous polarization is directed along the *a* axis; it is accompanied by a spontaneous shear strain ε_4. A unit cell of Rochelle salt contains four formula units.

According to the classical concepts, based on structural data of Frazer *et al.*,[1] the phase transitions in the Rochelle salt are pure order-disorder ones. The ferroelectric polarization used to be attributed to rotation of hydroxyl groups of tartrate complexes OH_5 between two equilibrium positions (see Ref.2). Each cell presumably contains four dipoles; the potential barrier between two equilibrium orientations of a dipole is asymmetric. The dipoles form two copenetrating sublattices, with local potentials which are the mirror reflections of each other. Therefore, even though in each sublattice dipoles are always ordered (nonzero sublattice polarization), the total polarization at certain temperatures can be absent. These assumptions form the Mitsui model,[3] usually used for the description of the Rochelle salt.

The actual situation is far more complicated, and the mechanism of the phase transitions in the Rochelle salt remains rather obscure. More recent neutron scattering data indicate that the OH_5 hydroxyl groups do not perform any orientational motion and therefore play little role in the phase transition, at least in deuterated Rochelle salt.[4,5] Furthermore, experimental facts suggest that the phase transitions in Rochelle salt are displacive[6,7] ones or of mixed order-disorder and displacive type.[8,9] According to x-ray scattering experiments,[10] spontaneous polarization in the Rochelle salt is created by cooperative displacements of tartrate molecules and water molecules in a frame of K and Na ions. Recently Hlinka *et al.*,[11] based on their x-ray diffraction data, proposed that it is the order-disorder motion of OH_9 and OH_{10} groups, coupled with the displacive vibrations of OH_8 groups, that is responsible for the phase transitions in the Rochelle salt, as well as for the spontaneous polarization. So far which atoms perform the order-disorder motion has not been definitively established.

Whichever atoms of the Rochelle salt play the role of ordering units, there is little doubt that their motion should be described within the Mitsui model.[3] This model can exhibit several types of temperature behavior. Depending on the values of its parameters, it can undergo, for instance, a single second order phase transition into the ferroelectric phase (observed in $RbHSO_4$), two second order phase transitions (Rochelle salt), etc.

Static dielectric properties of Rochelle salt have been extensively studied within the Mitsui model by Vaks,[12] Zeks *et al.*,[13] Mori,[14] Kalenik,[15] and others. Spontaneous polarization and static dielectric permittivity of pure and deuterated Rochelle salt have been calculated.

Within the same model Zeks *et al.*,[13,16] Mori,[14] and Levitskii and co-workers[17–19] explored the relaxation dynamics of the Rochelle salt. The temperature dependence of the relaxation times and dynamic permittivity in the Rochelle salt was calculated. It was obtained, however, that the relaxation time, exhibiting a critical slowing down at the Curie points, actually diverges at these points, whereas experiments[20] indicate that it should be large but remain finite. An infinite relaxation time yields a zero contribution of the ordering system to the permittivity and, thereby, an incorrect theoretical temperature dependence of the permittivity near the Curie points. Zeks *et al.*[13,16] calculated relaxation times for the Mitsui model with tunneling (sometimes included into consideration in order to describe the isotopic effects in Rochelle salt) and showed that the increase in the tunneling integral does not have much effect on the dynamic properties. This incorrect behavior persists even when using a higher-order, two-particle cluster approximation[19] for the short-range interactions.

It should be noted that the problem of the incorrect temperature dependence of the relaxation times and dynamic permittivity near the Curie points is absent in a nonpiezoelectric $RbHSO_4$, usually described by the same model. Here the inverse relaxation times and the contribution of the ordering subsystem to the dynamic permittivity (both theoretical and experimental) indeed vanish at the Curie point.[21–24]

A remedy to the above mentioned problem seems obvious. It is well known that the Rochelle salt is one of the strongest piezoelectrics. The piezoelectricity splits the static permittivities of clamped and free crystals. At the frequency of the measuring electric field above the frequency of the piezoelectric resonance, a clamped dielectric permittivity of the crystal is measured. A simple Mitsui model does not

distinguish between the free and clamped permittivities; in fact, the relaxation times and dynamic permittivity at high frequencies calculated within its framework correspond to a free crystal. Instead, like the static dielectric permittivity of a clamped crystal, the relaxation times calculated for a clamped crystal should be finite at the Curie points.

It is thus obvious that taking into account the piezoelectric effects within the Mitsui model can be fruitful. Also, a microscopic theory of the piezoelectric and elastic properties of the Rochelle salt is still missing. The aim of this work is to verify the usefulness of this approach.

II. DIELECTRIC, ELASTIC, PIEZOELECTRIC, AND THERMAL CHARACTERISTICS OF FERROELECTRICS WITH ASYMMETRIC DOUBLE-WELL POTENTIAL

We consider a two-sublattice piezoelectric order-disorder type system with an asymmetric double-well potential. We start with the conventional Mitsui model and modify it by taking into account the shear strain $\varepsilon_4=\varepsilon_{yz}$, which is either spontaneous in the ferroelectric phase or induced by piezoelectric coupling with an external electric field E_1 applied along the ferroelectric axis a.

The model states that the phase transitions are caused by the motion of certain dipoles in asymmetric double-well potentials with two different constants for the interaction between dipoles of the same sublattice and of different sublattices. We consider a system without tunneling, assuming that the isotopic effect in the Rochelle salt is due to changes in the interaction constants. The relative unimportance of tunneling effects here is indicated by the relaxational character of dielectric dispersion in a pure undeuterated Rochelle salt. The model Hamiltonian then reads

$$\hat{H}=\frac{N}{2}vc_{44}^{E0}\varepsilon_4^2-Nve_{14}^0\varepsilon_4E_1-\frac{N}{2}v\chi_{11}^{\varepsilon 0}E_1^2 - \frac{1}{2}\sum_{qq'}\sum_{ff'=1}^{2}R_{qq'}(ff')\frac{\sigma_{qf}}{2}\frac{\sigma_{q'f'}}{2}-\Delta\sum_q\left(\frac{\sigma_{q_1}}{2}-\frac{\sigma_{q_2}}{2}\right) -(\mu_1E_1-2\psi_4\varepsilon_4)\sum_q\sum_{f=1}^{2}\frac{\sigma_{qf}}{2}. \tag{2.1}$$

The three first terms in Eq. (2.1) represent the elastic, piezoelectric, and electric energies attributed to a host lattice in which potential the quasispin move (with the ''seed'' elastic constant c_{44}^{E0}, the coefficient of piezoelectric stress e_{14}^0, and dielectric susceptibility $\chi_{11}^{\varepsilon 0}$); $v\equiv\overline{v}k_B$ is the unit cell volume. In the fourth term in Eq. (2.1) $R_{qq'}(11)=R_{qq'}(22)=J_{qq'}$ and $R_{qq'}(12)=R_{qq'}(21)=K_{qq'}$ are the potentials of interaction between quasispins belonging to the same and to different sublattices, respectively. The quantity Δ describes the asymmetry of the double-well potential; μ_1 is the effective dipole moment. The last term in the Hamiltonian is an additional internal field produced by piezoelectric coupling with the shear strain ε_4; ψ_4 is the so-called deformational potential.

To derive the additional field one should start from a general microscopic term of the

$$H'=\sum_{qf}\sum_{nk}\sum_{i\alpha\beta}{}^{i}C_{fk}^{\alpha\beta}(qn)D_{qf}^{\alpha}\,{}^{i}u_{nk}^{\beta} \tag{2.2}$$

type, usually appearing in Hamiltonians of the piezoelectric order-disorder type systems, which take into account ionic vibrations of a host lattice.[12,25] This term describes a piezoelectric interaction of the dipole moments D_{qf}^{α} attributed to the ordering pseudospin system with components of the ionic displacements ($i=t$) or rotation ($i=r$) vectors ${}^{i}u_{nk}^{\alpha}$. The components of the dipole moments directed along the axis of spontaneous polarization are related to the pseudospin operators $D_{qf}^{x}\sim\sigma_{qf}$. In centrosymmetric crystals ${}^{i}C_{fk}^{\alpha}(qn)=0$. Here the indices nk denote the kth atom in the nth unit cell.

We can separate a uniform lattice deformation $\varepsilon_{\alpha\beta}$ (spontaneous or induced by external stress) from relative displacements of crystal sublattices ${}^{i}c_k^{\alpha}$:

$${}^{i}u_{nk}^{\alpha}=\sum_{\gamma}\varepsilon_{\alpha\gamma}R_{nk}^{0\gamma}+{}^{i}c_k^{\alpha}+{}^{i}\tilde{u}_{nk}^{\alpha},\quad\langle{}^{i}\tilde{u}_{nk}^{\alpha}\rangle=0. \tag{2.3}$$

Additional condition for ${}^{i}c_k^{\alpha}$ is an equation for new equilibrium ionic coordinates,[25] obtained in the mean field approximation

$$v\sum_{\alpha\gamma}{}^{i}d_{\alpha\gamma;\beta}^{k}\varepsilon_{\alpha\gamma}+\sum_{\alpha k'i'}{}^{ii'}D_{\alpha\beta}^{kk'}(0)\,{}^{i}c_{k'}^{\alpha}-\sum_{f\alpha}{}^{i}C_{fk}^{\alpha\beta}(0)\langle D_f^{\alpha}\rangle=0,$$

where ${}^{ii'}D_{\alpha\beta}^{kk'}(0)=\Sigma_n{}^{ii'}\Phi_{\alpha\beta}\binom{kk'}{nn'}$ is the dynamic matrix of the crystal, and ${}^{i}d_{\alpha\gamma;\beta}^{k'}=(1/v)\Sigma_{nk}{}^{ti}\Phi_{\alpha\beta}\binom{kk'}{nn'}R_{nk}^{0\gamma}$ (see a similar derivation for the case of KD_2PO_4 systems[25]). This equation is equivalent to the condition that the final Hamiltonian should not contain terms linear in ${}^{i}\tilde{u}_{nk}^{\alpha}$.

Taking into account only the shear strain $\varepsilon_4=\varepsilon_{yz}$, we arrive at the final expression for the additional field

$$H'=2\psi_4\varepsilon_4\sum_{qf}\frac{\sigma_{qf}}{2},$$

consistent with the system symmetry. Analogous fields induced by piezoelectric coupling with spontaneous shear strain ε_6 have been obtained also for the KD_2PO_4 type ferroelectrics,[25,26] and enabled a quantitative description of temperature behavior of elastic and piezoelectric characteristics of those crystals.[26]

Hereinafter we restrict our analysis to within the mean field approximation. Performing an identity transformation

$$\sigma_{qf}=\eta_f+(\sigma_{qf}-\eta_f),\quad\eta_f=\eta_{qf}=\langle\sigma_{qf}\rangle \tag{2.4}$$

and neglecting the quadratic fluctuations, we rewrite the initial Hamiltonian as

$$\hat{H}_m=\frac{N}{2}v c_{44}^{E0}\varepsilon_4^2-Nv e_{14}^0\varepsilon_4 E_1-\frac{N}{2}v\chi_{11}^{\varepsilon 0}E_1^2+\frac{N}{8}J(\eta_1^2+\eta_2^2)$$

$$+\frac{N}{4}K\eta_1\eta_2-\sum_q\left[E(1)\frac{\sigma_{q_1}}{2}-E(2)\frac{\sigma_{q_2}}{2}\right], \qquad (2.5)$$

where $J=\Sigma_q J_{qq'}$ and $K=\Sigma_q K_{qq'}$ are the Fourier transforms of the interaction constants at $\mathbf{q}=0$, whereas $E(1)$ and $E(2)$ are the local fields acting on the qth quasispin in the first and second sublattices, respectively

$$E(1)=\frac{1}{2}J\eta_1+\frac{1}{2}K\eta_2+\Delta-2\psi_4\varepsilon_4+\mu_1E_1,$$

$$E(2)=\frac{1}{2}J\eta_2+\frac{1}{2}K\eta_1-\Delta-2\psi_4\varepsilon_4+\mu_1E_1. \qquad (2.6)$$

Single-particle distribution functions of quasispins are

$$\eta_1=\tanh\left[\frac{\tilde{J}}{4T}\eta_1+\frac{\tilde{K}}{4T}\eta_2+\frac{\tilde{\Delta}}{2T}-\frac{\tilde{\psi}_4}{T}\varepsilon_4+\frac{\tilde{\mu}_1E_1}{2T}\right],$$

$$\eta_2=\tanh\left[\frac{\tilde{J}}{4T}\eta_2+\frac{\tilde{K}}{4T}\eta_1-\frac{\tilde{\Delta}}{2T}-\frac{\tilde{\psi}_4}{T}\varepsilon_4+\frac{\tilde{\mu}_1E_1}{2T}\right], \qquad (2.7)$$

where $\tilde{J}=J/k_B$, $\tilde{K}=K/k_B$, etc.

Introducing ferroelectric and antiferroelectric ordering parameters

$$\xi=\frac{1}{2}(\eta_1+\eta_2),\quad \sigma=\frac{1}{2}(\eta_1-\eta_2),$$

we obtain

$$\xi=\frac{\sinh\gamma}{\cosh\gamma+\cosh\delta},\quad \sigma=\frac{\sinh\delta}{\cosh\gamma+\cosh\delta}, \qquad (2.8)$$

where

$$\gamma=\beta\left(\frac{J+K}{2}\xi-2\psi_4\varepsilon_4+\mu_1E_1\right),$$

$$\delta=\beta\left(\frac{J-K}{2}\sigma+\Delta\right).$$

A trivial solution $\xi=0$ $(\eta_1=-\eta_2)$ at $E_1=0$ yields zero macroscopic polarization at nonzero sublattice polarizations.

The piezoelectric, elastic, and dielectric characteristics of Rochelle salt can be derived from the thermodynamic potential $g_{1E}(\sigma_4,T,E_1)$:

$$\frac{g_{1E}}{Nk_B}=\frac{1}{2}\overline{v}c_{44}^{E0}\varepsilon_4^2-\overline{v}e_{14}^0\varepsilon_4E_1-\frac{1}{2}\overline{v}\chi_{11}^{\varepsilon 0}E_1^2+\frac{1}{4}(\tilde{J}+\tilde{K})\xi^2$$

$$+\frac{1}{4}(\tilde{J}-\tilde{K})\sigma^2-2T\ln 2-T\ln\cosh\frac{1}{2}(\gamma+\delta)$$

$$-T\ln\cosh\frac{1}{2}(\gamma-\delta)-\overline{v}\sigma_4\varepsilon_4. \qquad (2.9)$$

Here σ_4 is the shear stress conjugate to the strain ε_4. In numerical calculations $\sigma_4=0$.

The conditions

$$\frac{1}{\overline{v}}\left(\frac{\partial g_{1E}}{\partial\varepsilon_4}\right)_{E_1,\sigma_4}=0,\quad \frac{1}{\overline{v}}\left(\frac{\partial g_{1E}}{\partial E_1}\right)=-P_1 \qquad (2.10)$$

yield

$$\sigma_4=c_{44}^{0E}\varepsilon_4-e_{14}^0E_1+2\frac{\psi_4}{\overline{v}}\xi,$$

$$P_1=e_{14}^0\varepsilon_4+\chi_{11}^{0\epsilon}E_1+\frac{\mu_1}{v}\xi. \qquad (2.11)$$

The second derivatives of thermodynamic potential (2.9) are the coefficient of the piezoelectric stress,

$$e_{14}=\left(\frac{\partial P_1}{\partial\varepsilon_4}\right)_{E_1}=e_{14}^0-\beta\psi_4\frac{\mu_1}{v}f_1(\xi,\sigma), \qquad (2.12)$$

the clamped static dielectric susceptibility

$$\chi_{11}^{\varepsilon}=\left(\frac{\partial P_1}{\partial E_1}\right)_{\varepsilon_4}=\chi_{11}^{\varepsilon 0}+\frac{\beta\mu_1^2}{2v}f_1(\xi,\sigma), \qquad (2.13)$$

and the elastic constant at constant field

$$c_{44}^E=\left(\frac{\partial\sigma_4}{\partial\varepsilon_4}\right)_{E_1}=c_{44}^{E0}-\frac{2\beta\psi_4^2}{v}f_1(\xi,\sigma), \qquad (2.14)$$

Inverting relations (2.11), we can express the strain ε_4 and field E_1 in terms of the polarization and stress and then find the coefficient of the piezoelectric strain

$$d_{14}=\left(\frac{\partial P_1}{\partial\varepsilon_4}\right)_{E_1}=d_{14}^0+\frac{s_{44}^{E0}\mu_1'\beta\psi_4}{v}f_2(\xi,\sigma), \qquad (2.15)$$

the dielectric susceptibility of a free crystal,

$$\chi_{11}^{\sigma}=\left(\frac{\partial P_1}{\partial E_1}\right)_{\sigma_4}=\chi_{11}^{\sigma 0}+\frac{\beta(\mu_1')^2}{2v}f_2(\xi,\sigma), \qquad (2.16)$$

and the elastic compliance s_{44}^E

$$s_{44}^E=\left(\frac{\partial\varepsilon_4}{\partial\sigma_4}\right)_{E_1}=s_{44}^{E0}+(s_{44}^{E0})^2\frac{2\beta\psi_4^2}{v}f_2(\xi,\sigma). \qquad (2.17)$$

Here

$$f_1(\xi,\sigma)=\frac{\rho+\frac{\tilde{K}-\tilde{J}}{4T}[\rho^2-4\xi^2\sigma^2]}{\left[1-\frac{\tilde{K}+\tilde{J}}{4T}\rho\right]\left[1+\frac{\tilde{K}-\tilde{J}}{4T}\rho\right]+\frac{\tilde{K}^2-\tilde{J}^2}{T}\xi^2\sigma^2},$$

$$f_2(\xi,\sigma)=\frac{\rho+\dfrac{\tilde{K}-\tilde{J}}{4T}[\rho^2-4\xi^2\sigma^2]}{[1-\rho\zeta]\left[1+\dfrac{\tilde{K}-\tilde{J}}{4T}\rho\right]+\zeta\dfrac{\tilde{K}-\tilde{J}}{T}\xi^2\sigma^2},$$

$$\rho=1-\xi^2-\sigma^2,\quad \zeta=\frac{\tilde{K}+\tilde{J}}{4T}+\frac{2}{v}\frac{\tilde{\psi}_4^2}{T}s_{44}^{E0},$$

$$s_{44}^{E0}=\frac{1}{c_{44}^{E0}},\quad d_{14}^0=\frac{e_{14}^0}{c_{44}^{E0}},$$

$$\chi_{11}^{\sigma 0}=\chi_{11}^{\varepsilon 0}+e_{14}^0 d_{14}^0,\quad \mu_1'=-2\tilde{\psi}_4 d_{14}^0+\mu_1.$$

The rest of the piezoelectric and elastic characteristics can be expressed via those found above: the elastic constant at constant polarization,

$$c_{44}^P=\left(\frac{\partial\sigma_4}{\partial\varepsilon_4}\right)_{P_1}=c_{44}^E+e_{14}h_{14}, \tag{2.18}$$

the constant of piezoelectric stress,

$$h_{14}=-\left(\frac{\partial E_1}{\partial\varepsilon_4}\right)_{P_1}=\frac{e_{14}}{\chi_{11}^{\varepsilon}}, \tag{2.19}$$

and the constant of piezoelectric strain,

$$g_{14}=\left(\frac{\partial E_1}{\partial\sigma_4}\right)_{P_1}=\frac{d_{14}}{\chi_{11}^{\sigma}}. \tag{2.20}$$

The temperature of the second order phase transition is determined from the condition that the dielectric susceptibility of a free crystal χ_{11}^{σ} diverges at $T\to T_{C1}$ and $T\to T_{C2}$,

$$\bar{t}_c^0-(1-\sigma^2)=0.$$

Using Eq. (2.16), we get

$$\frac{1}{\bar{t}_c^0}=\cosh^2\left(-\frac{\bar{a}}{\bar{t}_c^0}\sigma+\frac{\bar{b}}{\bar{t}_c^0}\right) \tag{2.21}$$

or

$$\cosh^2\left(-\frac{\tilde{K}-\tilde{J}}{4T_C}\sigma+\frac{\Delta}{2T_C}\right)=\frac{\tilde{K}+\tilde{J}}{4T_C}+\frac{2\tilde{\psi}_4^2 s_{44}^{E0}}{v T_C}.$$

Here we introduced the dimensionless variables $\bar{a}$, $\bar{b}$, and $\bar{t}^0$:

$$\bar{a}=\frac{\frac{1}{4}(\tilde{K}-\tilde{J})}{\frac{1}{4}(\tilde{K}+\tilde{J})+\frac{2}{v}\tilde{\psi}_4^2 s_{44}^{E0}},$$

$$\bar{b}=\frac{2\tilde{\Delta}}{\frac{1}{4}(\tilde{K}+\tilde{J})+\frac{2}{v}\tilde{\psi}_4^2 s_{44}^{E0}},$$

$$\bar{t}^0=\frac{T}{\frac{1}{4}(\tilde{K}+\tilde{J})+\frac{2}{v}\tilde{\psi}_4^2 s_{44}^{E0}}. \tag{2.22}$$

To calculate the thermal characteristics of the Rochelle salt we use the free energy

$$f=g_{1E}+\bar{v}P_1E_1+\bar{v}\sigma_4\varepsilon_4. \tag{2.23}$$

The specific heat of the quasispin subsystem of the Rochelle salt at constant stress σ_4 then reads

$$\Delta C^{\sigma}=-T\left(\frac{dS}{dT}\right)_{\sigma}=q_4^{P_1,\varepsilon_4}+q_{\xi}^{\varepsilon_4}p_{\xi}^{\sigma_4}+q_{\sigma}^{\varepsilon_4}p_{\sigma}^{\sigma_4}+q_4^p\alpha_4, \tag{2.24}$$

where

$$q_4^{P_1,\varepsilon_4}=T\left(\frac{\partial S}{\partial T}\right)_{P_1,\varepsilon_4}=R\left[(\gamma^2+\delta^2)\frac{\rho}{2}-2\gamma\delta\xi\sigma\right],$$

$$q_{\xi}^{\varepsilon_4}=T\left(\frac{\partial S}{\partial\xi}\right)_{\varepsilon_4,T}=\frac{v}{\mu_1}R\frac{\tilde{J}+\tilde{K}}{4}[-\gamma\rho+2\delta\xi\sigma],$$

$$q_{\sigma}^{\varepsilon_4}=T\left(\frac{\partial S}{\partial\sigma}\right)_{\varepsilon_4,T}=\frac{v}{\mu_1}R\frac{\tilde{J}-\tilde{K}}{4}[-\delta\rho+2\gamma\xi\sigma],$$

$$q_4^{P_1}=T\left(\frac{\partial S}{\partial\varepsilon_4}\right)_{P_1,T}=R\tilde{\psi}_4[\gamma\rho-2\delta\xi\sigma],$$

S is the molar entropy,

$$\frac{S}{R}=2\ln 2+\ln\cosh\frac{1}{2}(\gamma+\delta)+\ln\cosh\frac{1}{2}(\gamma-\delta)-\gamma\xi-\delta\sigma,$$

and α_4 is the coefficient of the thermal expansion:

$$\alpha_4=\left(\frac{\partial\varepsilon_4}{\partial T}\right)_{\sigma_4}=\frac{-p_4+h_{14}p_{\xi}^{\varepsilon_4}}{c_{44}^E}. \tag{2.25}$$

Rather cumbersome expressions for p_4 and $p_{\xi}^{\varepsilon_4}$ are given in the Appendix. The pyroelectric coefficient reads

$$p_4^{\sigma_4}=-\left(\frac{\partial P_1}{\partial T}\right)_{\sigma_4}=-(p_{\xi}^{\varepsilon_4}+e_{14}\alpha_4). \tag{2.26}$$

III. RELAXATION DYNAMICS

Dynamic properties of the system with Hamiltonian (2.1) are studied within the Glauber method.[27] For a complete statistical description of a quasispin subsystem dynamics, one

needs to know the probabilities $P\{\ldots,\sigma_{qf},\ldots\}$ that the quasispins are in the state $\{\ldots,\sigma_{qf},\ldots\}$ at time t. It is assumed that the time dependence of this probability function is given by the master equation[27]

$$\frac{d}{dt}P\{\ldots,\sigma_{qf},\ldots\} = -\sum_q w_q\{\ldots,\sigma_{qf},\ldots\}P\{\ldots,\sigma_{qf},\ldots\} + \sum_q w_q\{\ldots,-\sigma_{qf},\ldots\}P\{\ldots,-\sigma_{qf},\ldots\}. \tag{3.1}$$

Here $w_q\{\ldots,\sigma_{qf},\ldots\}$ is the probability that, due to a contact with a heat reservoir, the qfth quasispin flips from the state σ_{qf} to the state $-\sigma_{qf}$ within the unit time. It is assumed that the heat reservoir is always in equilibrium, or that there exists a mechanism which returns it to equilibrium sufficiently fast. The function $w_q\{\ldots,\sigma_{qf},\ldots\}$ should have the form ensuring a transition from the stochastic model to the equilibrium configuration described by Hamiltonian (2.1).

From the detailed balancing condition at equilibrium

$$\frac{w_{qf}\{\ldots,\sigma_{qf},\ldots\}}{w_{qf}\{\ldots,-\sigma_{qf},\ldots\}} = \frac{P_0\{\ldots,-\sigma_{qf},\ldots\}}{P_0\{\ldots,\sigma_{qf},\ldots\}}$$

[here $P_0\{\ldots,\sigma_{qf},\ldots\}$ is the equilibrium distribution function, being proportional to the Maxwell-Boltzmann factor $\exp(-\beta\hat{H})$] the expression for the spin flopping probability $w_{qf}\{\ldots,\sigma_{qf},\ldots\}$ follows:

$$w_{qf}\{\ldots,\sigma_{qf},\ldots\} = \frac{1}{2\alpha}\left[1-\sigma_{qf}\tanh\frac{1}{2}\beta E_{qf}\right]. \tag{3.2}$$

The parameter α describes the time scale on which all transitions in the system take place, E_{qf} denotes the operator field acting on the qf-th spin; in the mean field approximation the fields are given by Eq. (2.6).

To solve the master equation is quite a complicated task. Fortunately, we may considerably simplify it, by looking not for the probability function $P(\ldots,\sigma_{qf},\ldots)$, but for the expectation values of spins products

$$\left\langle \prod_f \sigma_{qf} \right\rangle = \sum_{\{\sigma\}} \prod_f \sigma_{qf} P\{\ldots,\sigma_{qf},\ldots,t\}$$

(the sum is carried out over the all 2^N system configurations). The equations for such expectation values follow from the master equation and from Eq. (3.2):

$$-\alpha\frac{d}{dt}\left\langle \prod_f \sigma_{qf} \right\rangle = \sum_f \left\langle \prod_{f'} \sigma_{qf'}\left[1-\sigma_{qf}\tanh\frac{1}{2}\beta E_{qf}\right]\right\rangle.$$

The sum here is carried out only over the spins that occur in the product $\Pi_{f'}$.

Within this approach, the system of equations for the time-dependent single-particle distribution functions is obtained as

$$-\alpha\frac{d}{dt}\xi = \xi - \frac{1}{2}\left(\tanh\frac{1}{2}(\gamma+\delta)+\tanh\frac{1}{2}(\gamma-\delta)\right),$$

$$-\alpha\frac{d}{dt}\sigma = \sigma - \frac{1}{2}\left(\tanh\frac{1}{2}(\gamma+\delta)-\tanh\frac{1}{2}(\gamma-\delta)\right). \tag{3.3}$$

At small deviations of the system from equilibrium, we can present ξ and σ as the sums of two terms each: equilibrium functions and their deviations from the equilibrium values:

$$\xi = \tilde{\xi}+\xi_t, \quad \sigma = \tilde{\sigma}+\sigma_t. \tag{3.4}$$

An essential point of the derivation is that the strain ε_4 is assumed to be time independent, which is the case above the piezoelectric resonance frequency. In a rather wide temperature range, provided the deviations from equilibrium are small, we can expand the system (3.3) coefficients into Taylor series in ξ_t, σ_t, and E_t up to the linear terms. The system then splits into two groups of systems: one for the equilibrium functions [this system coincides with Eq. (2.8)] and one for their fluctuation parts:

$$-\alpha\frac{d}{dt}\xi_t = a_{11}\xi_t + a_{12}\sigma_t + \frac{\mu_1 E_1}{2T}a_1,$$

$$-\alpha\frac{d}{dt}\sigma_t = a_{21}\xi_t + a_{22}\sigma_t + \frac{\mu_1 E_1}{2T}a_2. \tag{3.5}$$

Here we use the notations

$$a_{11} = 1-\frac{\tilde{J}+\tilde{K}}{T}\frac{1-\cosh\gamma\cosh\delta}{(\cosh\gamma+\cosh\delta)^2},$$

$$a_{12} = \frac{\tilde{J}-\tilde{K}}{T}\frac{\sinh\gamma\sinh\delta}{(\cosh\gamma+\cosh\delta)^2},$$

$$a_{21} = \frac{\tilde{J}+\tilde{K}}{T}\frac{\sinh\gamma\sinh\delta}{(\cosh\gamma+\cosh\delta)^2},$$

$$a_{22} = 1-\frac{\tilde{J}-\tilde{K}}{T}\frac{1-\cosh\gamma\cosh\delta}{(\cosh\gamma+\cosh\delta)^2},$$

$$a_1 = \frac{4(1-\cosh\gamma\cosh\delta)}{(\cosh\gamma+\cosh\delta)^2},$$

$$a_2 = \frac{4\sinh\gamma\sinh\delta}{(\cosh\gamma+\cosh\delta)^2}.$$

At $E_t=0$ from Eqs. (3.5) we obtain a uniform differential equation for ξ_t:

$$\ddot{\xi}_t - K_1\dot{\xi}_t + K_0\xi_t = 0. \tag{3.6}$$

Here $K_1 = a_{11}+a_{22}$, $K_0 = \left|\begin{smallmatrix} a_{11} & a_{12} \\ a_{21} & a_{22}\end{smallmatrix}\right|$. Its general solution reads

$$\xi_t = C_1^\tau \exp(-t/\tau_1) + C_2^\tau \exp(-t/\tau_2), \tag{3.7}$$

where C_f^τ are constant coefficients, and τ_f are relaxation times

$$\tau_{1,2}^{-1} = \frac{1}{2}\{K_1 \pm \sqrt{K_1^2 - 4K_0}\}. \tag{3.8}$$

Solving the nonuniform system of equations (3.5), we obtain [the electric field is $E_t = E_0 \exp(i\omega t)$]

$$\xi_t = \sum_{f=1}^{2} C_f^\tau \exp(-t/\tau_f) + \frac{i\omega K^{(1)} + K^{(0)}}{(i\omega)^2 - i\omega K_1 + K_0} \frac{\mu_1 E_t}{2k_B T},$$

where $K^{(1)} = -a_1$, $K^{(0)} = -\left|\begin{smallmatrix} a_{12} & a_1 \\ a_{22} & a_2 \end{smallmatrix}\right|$.

The complex dielectric permittivity then reads

$$\varepsilon'_{11}(\omega) = \varepsilon_\infty + \frac{4\pi\chi_1}{1+(\omega\tau_1)^2} + \frac{4\pi\chi_2}{1+(\omega\tau_2)^2},$$

$$\varepsilon''_{11}(\omega) = \frac{4\pi\chi_1\omega\tau_1}{1+(\omega\tau_1)^2} + \frac{4\pi\chi_2\omega\tau_2}{1+(\omega\tau_2)^2}. \tag{3.9}$$

where

$$\chi_{1,2} = \frac{\beta\mu_1^2}{2v} \frac{\tau_1\tau_2}{\tau_2 - \tau_1}(\mp K^{(1)} \pm \tau_1 K^{(0)}). \tag{3.10}$$

IV. DISCUSSION

A. Fitting procedure

All the subsequent calculations refer to the undeuterated Rochelle salt. For the numerical description of the above calculated dielectric, piezoelectric, elastic, thermal, and relaxational characteristics, we need to set the values of the following theory parameters: interaction potentials in the same and in different sublattices $\tilde{J}$ and $\tilde{K}$; the asymmetry parameter $\tilde{\Delta}$, deformational potential $\tilde{\psi}_4$; effective dipole moment μ_1; the quantity α that sets a time scale of dynamic processes in the system; the ''seed'' elastic constant c_{44}^{E0}, dielectric susceptibility $\chi_{11}^{\sigma 0}$, the coefficient of the piezoelectric strain, d_{14}^0; and the unit cell volume v.

The number and temperatures of the second order phase transitions in the considered system are governed by the dimensionless parameters $\bar{a}$ and $\bar{b}$ [Eq. 2.21)]. A thorough study of the phase diagram of the conventional Mitsui model has been recently presented elsewhere[24,28] (also see Ref. 12). Several new regions in the diagram (missed in the earlier studies[12] of the model) were revealed, where the system without tunneling can undergo up to four different phase transitions. Inclusion of the piezoelectric effects into the model does not affect the topology of the phase diagram and only renormalizes the parameters $\bar{a}$ and $\bar{b}$.

In the $(\bar{a}, \bar{b})$ phase diagram of the model,[24,12] only a single line corresponds to the Rochelle salt. Two second order phase transitions occur along this line, and the ratio of the transition temperatures coincides with that observed experimentally in the Rochelle salt: $T_{C1}/T_{C2} = 255/297 \approx 0.86$.

On lowering $\bar{a}$ and $\bar{b}$ along this line, the maximum value of ξ between the two Curie points increases. At some point, however, a third phase transition of the first order into a ferroelectric phase emerges at $T \approx 0$ K, in addition to the known transitions at T_{C1} and T_{C2}. The temperature of the third transition increases on further decreasing of $\bar{a}$ and $\bar{b}$. There is some experimental evidence that such a transition indeed takes place in Rochelle salt at a temperature around 212 K (see Ref. 29 and references therein), but in the present paper we restrict our consideration to the commonly accepted case of two phase transitions.

In order to obtain the best description of the spontaneous polarization (see below) we choose the values of $\bar{a} = 0.295$ and $\bar{b} = 0.648$ corresponding to the terminating point of the Rochelle salt line, where the maximum value of ξ is the largest, and the system still undergoes only two second order phase transitions. Knowing the dimensionless temperatures t_C^0 of the two transitions, we can unambiguously find $\tilde{J}, \tilde{K}$, and $\tilde{\Delta}$ from Eqs. (2.22), provided the parameters $\tilde{\psi}_4$ and c_{44}^{E0} are chosen. The deformation potential $\tilde{\psi}_4$ and the seed elastic constant c_{44}^{E0} can be found by fitting the theoretical temperature dependence of the elastic constant to the experimental[30] one. Hence, checking several trial values of $\tilde{\psi}_4$ and c_{44}^{E0}, we find $\tilde{J}, \tilde{K}$, and $\tilde{\Delta}$.

As a result, $\tilde{J} = 797.36$ K, $\tilde{K} = 1468.83$ K, $\tilde{\Delta} = 737.33$ K, $\tilde{\psi}_4 = -760$ K, and $c_{44}^{E0} = 12.8 \times 10^{10}$ dyn/cm^2.

The effective dipole moment μ_1 is set by fitting to the experimental values[20] of the static dielectric permittivity of a clamped crystal at the transition points. In the subsequent calculations, we consider the moment μ_1 to be a slightly decreasing function of temperature

$$\mu_1 = [2.52 + 0.0066(297 - T)] \times 10^{-18} \text{esu cm}$$

The value of $\alpha = 1.7 \times 10^{-13}\ c^{-1}$ is obtained by fitting the theoretical value of $\varepsilon'_{11}(\nu, T)$ at $\nu = 2.5$ GHz at the upper Curie point to the experimental one.[20] The ''seed'' quantities $\chi_{11}^{\sigma 0} = 0.363$ and $d_{14}^0 = 1.9 \times 10^{-8}$ esu/dyn are taken to be equal to the experimental values of χ_{11}^σ (Ref. 31) and d_{14} (Ref. 32) at $T > 320$ K.

The unit cell of the considered model contains only *two* ordering units. Following the usual practice of assuming that the actual unit cell of the Rochelle salt crystal contains *four* dipoles (one per molecule), we should set the value of the model unit cell volume v to be half of the crystal unit cell volume. Using the data of Ref. 33 we have

$$v = 0.5219[1 + 0.00013(T - 190)] \times 10^{-21}\ \text{cm}^3.$$

B. Static dielectric properties

Theoretical dependence of spontaneous polarization P_1 of the Rochelle salt is presented in Fig. 1. The obtained curve for $P_1(T)$ is somewhat asymmetric because μ_1 is taken as a decreasing function of temperature. Even though we chose

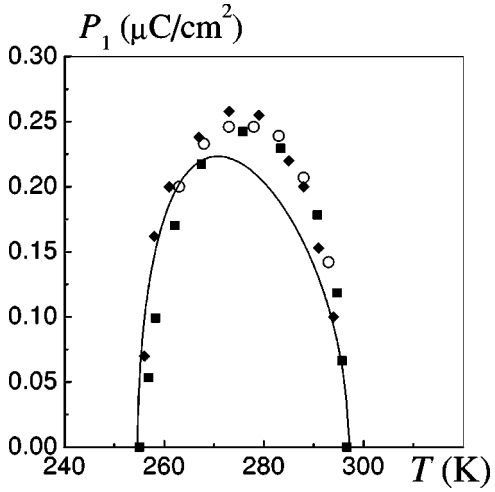

FIG. 1. Temperature dependence of spontaneous polarization: ○ (Ref. 34); ■ (Ref. 31); and ◇ (Ref. 35).

those values of the parameters $\bar{a}$ and $\bar{b}$ that yield the maximum values of ξ and P_1, the theoretical value of the spontaneous polarization is about 10% smaller than the experimental one. Later we shall discuss the ways to improve the agreement.

In Fig. 2 we show the calculated theoretical temperature dependences of inverse static dielectric susceptibilities of free $(\chi_{11}^{\sigma})^{-1}$ and clamped $(\chi_{11}^{\varepsilon})^{-1}$ Rochelle salt crystals. As one can see, the value of the effective dipole moment μ_1 chosen via two experimental points for dynamic clamped susceptibility at Curie temperatures, also provides a good fit to the inverse free susceptibility in the upper paraelectric phase. It should be noted that the temperature behavior of the inverse susceptibility in this phase is essentially non-linear, and the Curie-Weiss law here is a very poor approximation.

In the low temperature paraelectric phase the theoretical line noticeably deviates from most of experimental points for the free susceptibility. As will be shown below, a similar deviation also takes place for the other static and dynamic characteristics. While for piezoelectric and dielectric ones we could improve the agreement between theory and experiment by assuming a fancier temperature dependence of the effective dipole moment μ_1 (say, with bends at the Curie points), the discrepancy for the elastic constant c_{44}^{E}, which does not depend on μ_1, would persist. So far we have no solution to this problem.

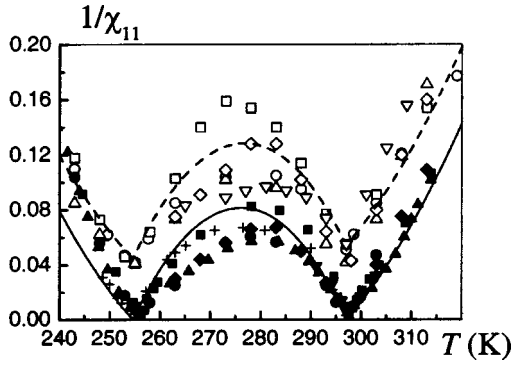

FIG. 2. Temperature dependence of inverse static dielectric susceptibility of a free crystal: [■ (Ref. 31), ▲ (Ref. 36), ♦ (Ref. 35), ● (Ref. 37), ▼ (Ref. 38), + (Ref. 39)] and a clamped crystal [□ (Ref. 20), ○ (Ref. 40), ◇ (Ref. 35), △ (Ref. 41), and ▽ (Ref. 42)].

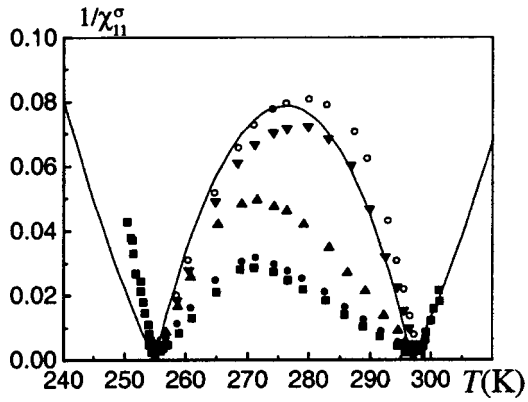

FIG. 3. Low-frequency dynamics of the inverse dielectric susceptibility as a function of temperature at different frequencies (Hz): ■, 0; ●, 1; ▲, 10; ▼, 80; ○, 1000. Experimental points are taken from Ref. 43. The solid line is a theoretical inverse static dielectric susceptibility of a free crystal.

In the ferroelectric phase, the frequency dispersion of dielectric susceptibility is observed[43] in the region below 1 kHz. This dispersion is attributed to the domain wall motion[43] or to the processes of domain polarization switching coupled to heat diffusion.[44] Experimental points[43] for the low-frequency dynamics in the Rochelle salt along with the theoretical line for a single-domain crystal are shown in Fig. 3. Increasing the frequency up to 1 kHz suppresses the dispersion[43]; this frequency is then considered as a high-frequency limit of this dynamics, where the domain effects are no longer essential. The theoretical single domain line fits best the points for 1 kHz, which also confirms the domain origin of the low-frequency dynamics.

C. Dynamic permittivity

Let us consider now the high-frequency relaxational properties of the Rochelle salt. In order to find out to what extent the experimental data of different sources for the dynamic permittivity $\varepsilon_{11}^{*}(\nu,T)$ agree, we plot the frequency dependences of these quantities at two temperatures in each of the three phases (see Figs. 4). The presented graphs reveal the relaxational dispersion of dielectric permittivity in the Rochelle salt. As one can see, the data of Refs. 20 and 46–48 agree fairly well and are sufficiently well described by the presented theory. Perceptible deviation is observed for rather outdated data of Ref. 41, where the frequency curve for $\varepsilon_{11}'(\nu,T)$ in the dispersion region is shifted to lower frequencies compared to the experimental points obtained in subsequent measurements. This indicates that the relaxation time obtained in Ref. 41 is much lower than in other papers.

In Fig. 5 we depict the calculated temperature dependence of the inverse relaxation times τ_1^{-1} and τ_2^{-1} along with the values of τ_1^{-1} obtained from the analysis of experimental

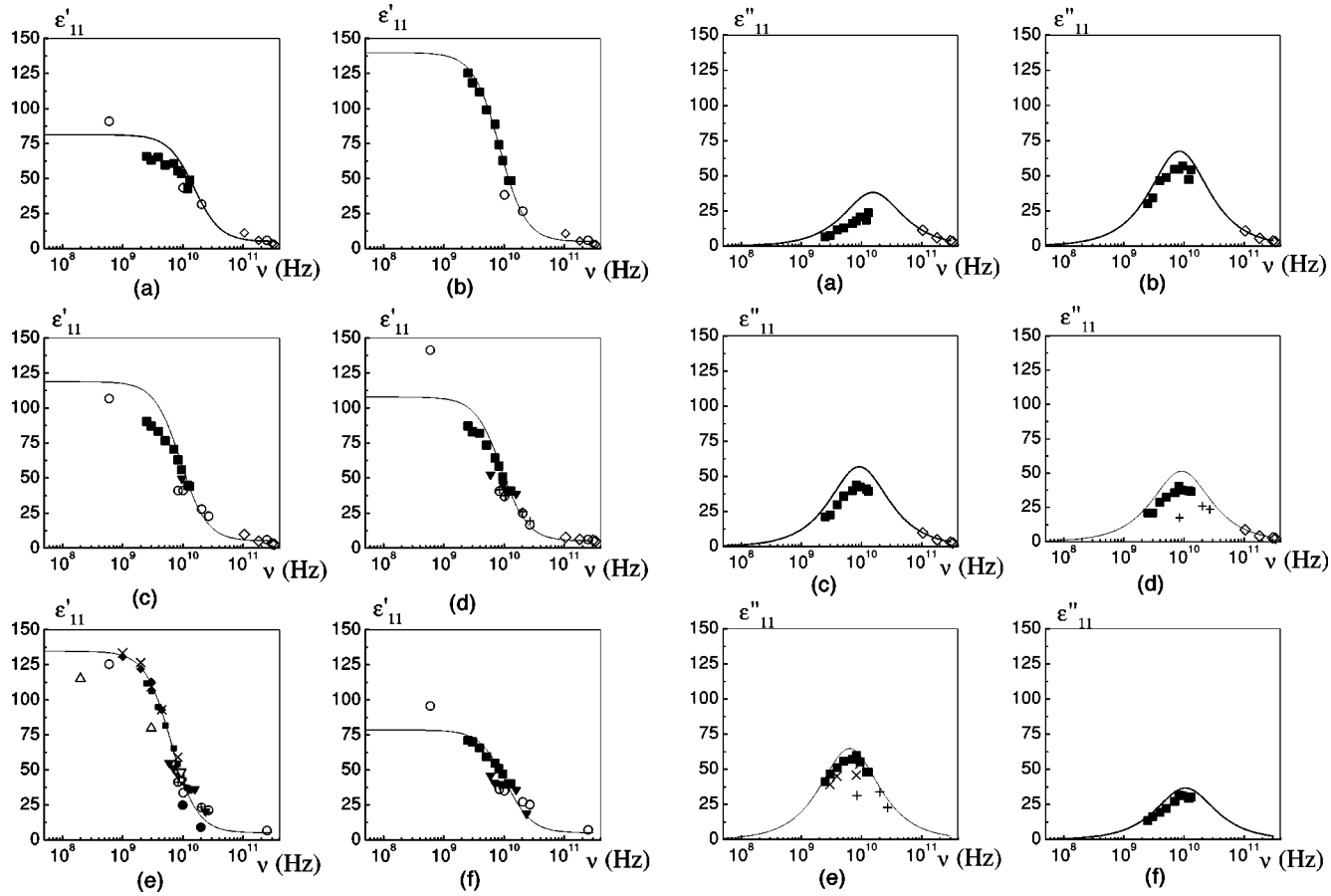

FIG. 4. The frequency dependence of the real and imaginary parts of dynamic dielectric permittivity at different temperatures T (K): (a) 235, (b) 245, (c) 265, (d) 285, (e) 305, and (f) 315. Experimental points are taken from ■ (Ref. 20), ○ (Refs. 45 and 49), + (Ref. 50), ▼ (Ref. 51), ● (Ref. 41), ◆ (Ref. 46), × (Ref. 47), ◇ (Ref. 48), △ (Ref. 38), and ▽ (Ref. 52).

data[20,41,46–48] for $\varepsilon_{11}^{*}(\nu,T)$. The recent data of Refs. 20, and 46–48 are well described by the presented theory.

As one can see, taking into account the piezoelectric effect has successfully solved the problem encountered by the conventional theories – incorrect temperature dependence of relaxation times near the Curie points. The theoretical temperature curve of $\tau_1^{-1}(T)$ obtained here has two *finite* minima at the transition points, as opposed to vanishing of the the inverse relaxation time obtained within the Mitsui model that does not take into account the piezoelectric effect.[13] The second relaxation time τ_2 is two orders smaller than τ_1 and does not exhibit any critical behavior. Moreover, the corresponding weight χ_2 [Eq. (3.10)] is different from zero only in the ferroelectric phase (this can be easily verified analytically) and even in this phase it is five orders smaller than χ_1. Therefore, the dielectric relaxation in this system is of Debye character, and its temperature behavior is determined by τ_1 and χ_1 only.

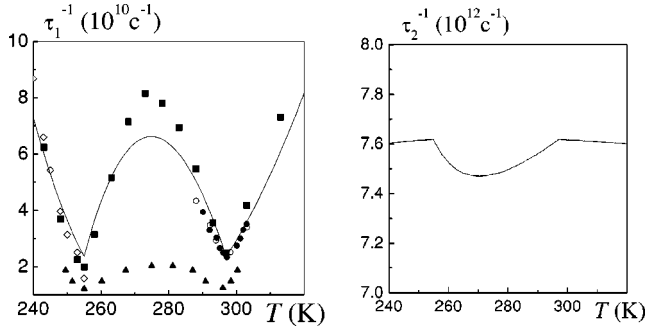

FIG. 5. Temperature dependence of the inverse relaxation times: ● (Ref. 46), ○ (Ref. 47), ■ (Ref. 20), ◇ (Ref. 48), and ▲ (Ref. 41).

Below we present the theoretical temperature dependences of $\varepsilon_{11}^{*}(\nu,T)$ along with the experimental points of Refs. 20 (Fig. 6), 47 (Fig. 7), and 46 (Fig. 8). The dielectric permittivity $\varepsilon'_{11}(\nu,T)$ has two extrema at the transition points T_{C2} and T_{C1}: maxima at lower frequencies $[\varepsilon'_{11}(\nu,T_{C1}) > \varepsilon'_{11}(\nu,T_{C2})]$ whose magnitudes decrease with increasing frequency; at $\nu > 4$ GHz narrow minima of $\varepsilon'_{11}(\nu,T)$ emerge within the broad peaks around T_{C1} and T_{C2}.

A fair quantitative description of experimental data is obtained, especially in the upper paraelectric phase. Note that the correct temperature behavior of the relaxation times in the vicinity of the Curie points yields correct behavior of the dynamic dielectric permittivity. However, we again notice a deviation from experimental data in the lower paraelectric phase.

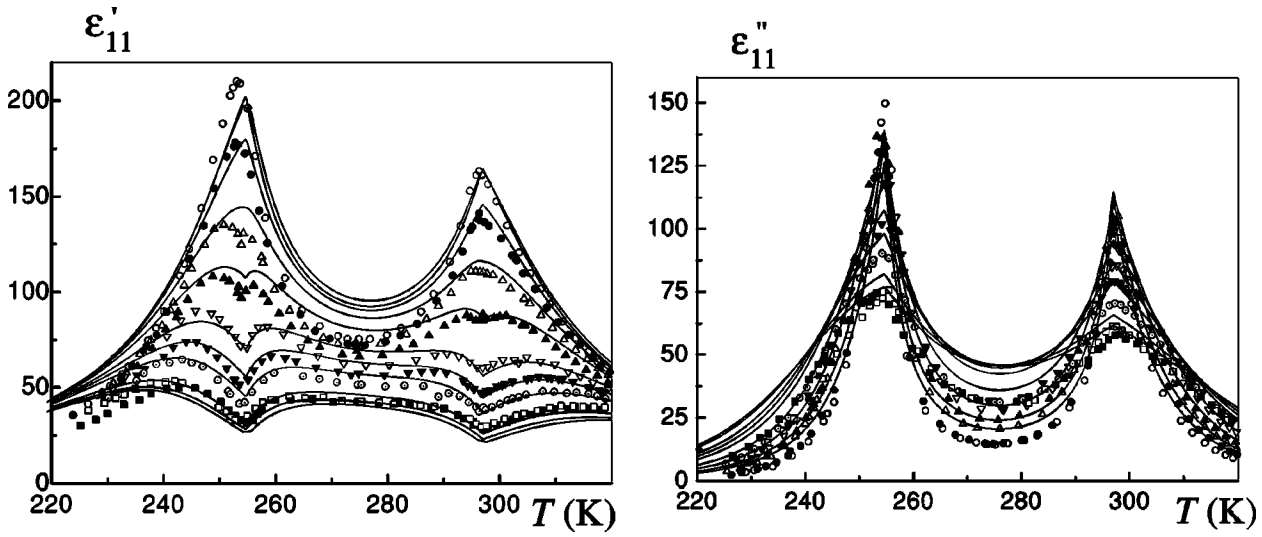

FIG. 6. The temperature dependence of the real and imaginary parts of the dynamic dielectric permittivity at different frequencies ν (GHz): ○, 2.5; ●, 3; △, 3.9; ▲, 5.1; ▽, 7.05; ▼, 8.25; ⊙, 9.45; □, 11.96; ■, 12.95. Solid lines are theoretical results; the symbols are experimental points taken from Ref. 20.

D. Elastic and piezoelectric properties

Let us now examine how the developed model describes the temperature behavior of the elastic and piezoelectric characteristics of the Rochelle salt associated with the strain ε_4. In Fig. 9 we present the theoretical temperature dependence of the elastic constants at constant field c_{44}^E and at constant polarization c_{44}^P. The calculated elastic constant c_{44}^P is almost temperature independent in all phases. On the contrary, the elastic constant c_{44}^E strongly depends on temperature, approaching zero at the Curie points. The results of the theoretical calculations for c_{44}^E agree well with the data of all measurements in the high-temperature paraelectric phase and with the data of Refs. 53 and 54, and 30 in the ferroelectric phase.

The theoretical rates of decrease of c_{44}^E as the temperature approaches the Curie points are the same in both paraelectric phases. However, the experimental data indicate that this rate is somewhat larger in the low-temperature paraelectric phase than in the high-temperature phase – we again obtain a deviation from the experiment in the low-temperature paraphase.

The temperature dependences of the piezoelectric characteristics of Rochelle salt are shown in Figs. 10–13. The calculated coefficient of piezoelectric strain d_{14} sharply increases as temperature approaches the transition points and diverges at $T=T_{Cf}$. The temperature dependence of e_{14} is weaker than that of d_{14}; at the transition points e_{14} has only finite maximum values. The constants of piezoelectric stress

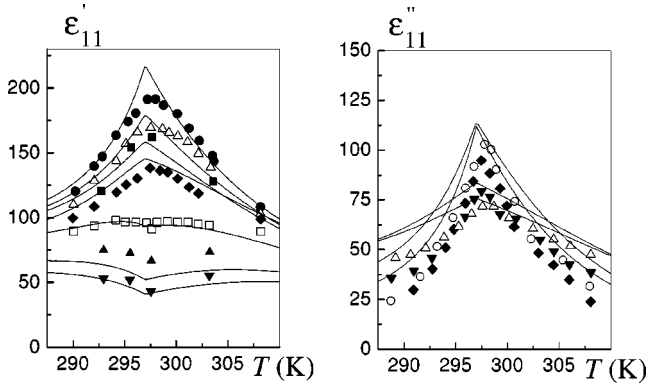

FIG. 7. The temperature dependence of the real and imaginary parts of the dynamic dielectric permittivity at different frequencies ν (GHz): ●, 1; △, 2; ■, 2.5; ◇, 3; □, 4.5; ▲, 7; ▼, 8.25. Experimental points are taken from Ref. 47.

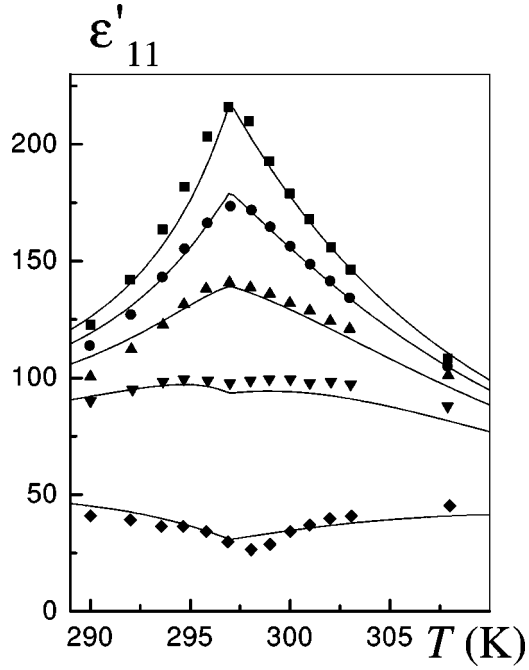

FIG. 8. The temperature dependence of the real part of the dynamic dielectric permittivity at different frequencies ν (GHz): ■, 1; ●, 2; ▲, 3; ▼, 4.5; ◇, 10. Experimental points are taken from Ref. 46.

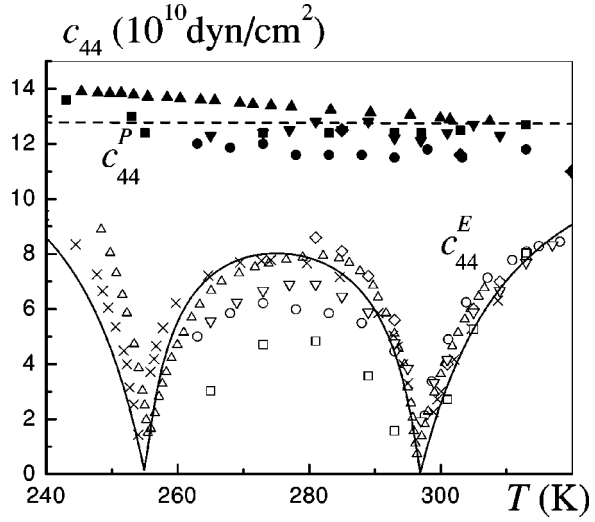

FIG. 9. Temperature dependence of elastic constant at constant field c_{44}^E [× (Ref. 30), △ (Ref. 53), ◇ (Ref. 54), ○, $1/s_{44}^E$ (Ref. 35), ▽, $1/s_{44}^E$ (Ref. 42) □ $c_{44}^P - e_{14}h_{14}$ (Refs. 37 and 57)] and constant polarization c_{44}^P [▲ (Ref. 53), ■ (Ref. 37), ◇ (Ref. 34), ● $1/s_{44}^E + e_{14}h_{14}$ (Ref. 35), ▼ $1/s_{44}^E + e_{14}^2/\chi_{11}^\varepsilon$ (Ref. 42)].

h_{14} and piezoelectric strain g_{14} hardly change with temperature and, therefore, are called ''true'' piezoelectric constants of a crystal.

The obtained curve $d_{14}(T)$ agrees well with the data of Refs. 42, and 44,55–57, and can be described by the Curie-Weiss law with B somewhat larger than those presented in Ref. 34. The coefficients e_{14}, h_{14}, and g_{14} are usually recalculated via the measured values of d_{14}, χ_{11}^σ, and c_{44}^E. Figures 11–13 contain ''experimental'' points obtained from such calculations. The theoretical results for e_{14} agree fairly well with the points obtained in Refs. 35, 42, and 57 but not in Ref. 37. Overall, more recent experimental data are better described by the presented theory. At any rate, the deviation of the theory from experiment does not exceed dispersion of experimental points from different sources.

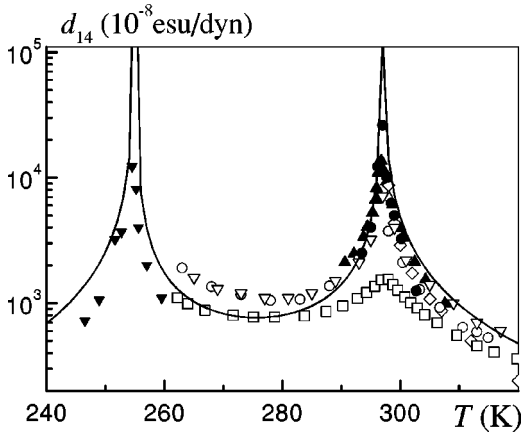

FIG. 10. Temperature dependence of the coefficient of piezoelectric strain d_{14}: ● (Ref. 55), ▲ (Ref. 32), ▼ (Ref. 56), □ (Ref. 37), ○ (Ref. 35), ▽ (Ref. 42), △ (Ref. 57), ◇ $d_{14}=B/(T-T_{C2})$, $B=8.67\times10^{-5}$ esu at $T<307$ K and 5.17×10^{-5} esu at $T>307$ K (Ref. 34).

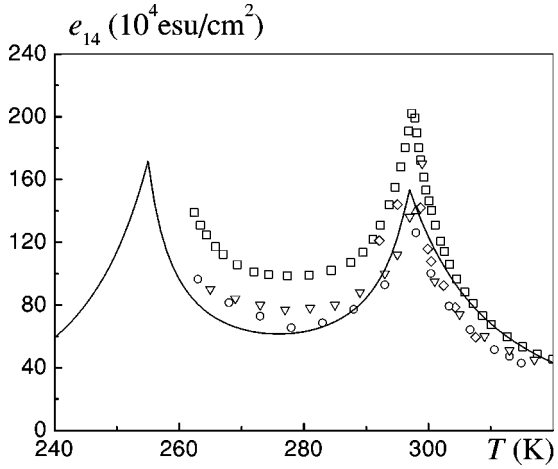

FIG. 11. Temperature dependence of the coefficient of the piezoelectric stress e_{14}: □ (Ref. 37), △ (Ref. 57), ▽ (Ref. 42), ○ (Ref. 35), ◇ $d_{14}\cdot c_{44}^E$ (Refs. 33 and 44).

E. Specific heat

Experimental data concerning the character of the anomalies of the specific heat of a Rochelle salt in the vicinity of the transition points are very controversial. The disagreement is caused by a small magnitude of the anomalies of specific heat that is not much larger than the dispersion of the obtained data. There were reported positive[29,59,60] (fast increase in the lower paraelectric phase and a downward jump at the transition point) or negative[61,62] (decrease and upward jump) anomalies of C^σ at the lower Curie point. At the upper Curie point a positive anomaly[29,59–62] or no anomaly at all[63] (in less precise measurements) was found. The most recent data show positive anomalies at both transition points. The same behavior is also predicted by the estimates made from the data of electrocaloric and piezocaloric measurements.[64,65]

Theoretical calculations yield two positive anomalies of the specific heat in a Rochelle salt. In Fig. 14 we plot the temperature dependence of the contribution to the specific heat from ordering quasispins ΔC^σ. This also agrees with the previous calculations,[19,24,66] where a similar temperature dependence of ΔC^σ was obtained within a model that does not take into account piezoelectric strain ε_4.

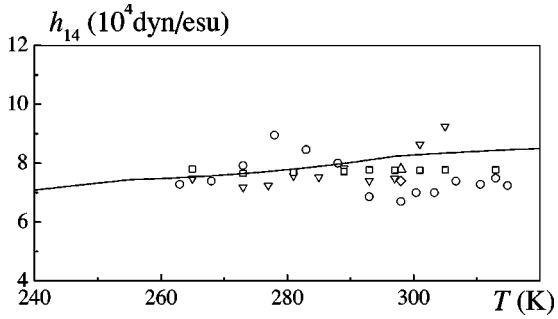

FIG. 12. Temperature dependence of the constant of piezoelectric stress h_{14}: □ (Ref. 37), △ (Ref. 57), ○ (Ref. 35), ▽ $e_{14}/\chi_{11}^\varepsilon$ (Ref. 42), and ◇ (Ref. 34).

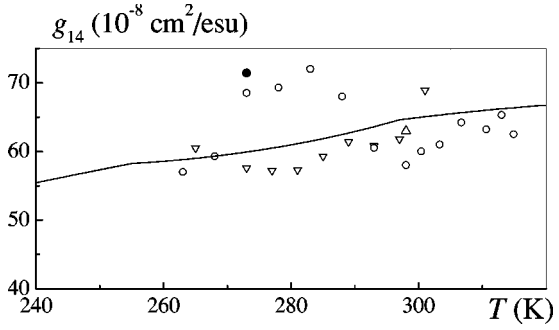

FIG. 13. Temperature dependence of the constant of piezoelectric strain g_{14}: △ (Ref. 57), ○ (Ref. 35), ▽ $d_{14}/\chi_{11}^{\varepsilon}+e_{14}d_{14}$ (Ref. 42), ● ε_4/P_1 (Refs. 58 and 31).

V. CONCLUSIONS

In the present paper we modified the Mitsui model for Rochelle salt crystals by taking into account the piezoelectric effects. The modified model successfully describes the piezoelectric and elastic characteristics of the Rochelle salt. It also predicts a correct temperature dependence of the relaxation times and dynamic dielectric permittivity near the Curie points. Since the clamped and free permittivities are now distinct, the relaxation times and dynamic dielectric permittivity calculated for the clamped crystal case remain finite at these points.

An unresolved problem is to obtain a simultaneous fit to spontaneous polarization in the ferroelectric phase and the second order dielectric and piezoelectric characteristics – the permittivities and piezoelectric modules in the paraelectric (antiferroelectric) phases with a single value of effective dipole moment μ. We can think of the following approaches to this problem.

(i) Take into account the electrostrictive forces.

(ii) Extend the model from the order-disorder one to a mixed displacive and order-disorder one, that is, to explicitly take into account the coupling with the displacive lattice mode(s), whose eigenvectors give rise to spontaneous polarization.

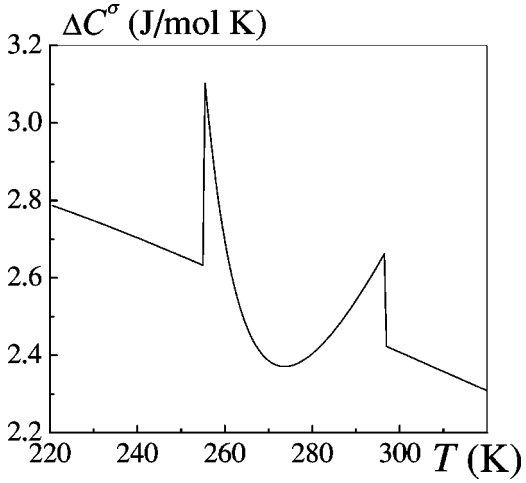

FIG. 14. Temperature dependence of ΔC^{σ}.

(iii) To assume that the number of ordering units per actual unit cell of the Rochelle salt is 8 rather than 4, as is usually taken now. This would halve the unit cell volume v entering the expressions for the polarization and dielectric permittivity. To keep the ratio μ_1^2/v equal to the value that provides an agreement with the permittivity, we should decrease the effective dipole moment by a factor of $\sqrt{2}$. The ratio μ_1/v entering the expression for spontaneous polarization is then increased by the same factor $\sqrt{2}$. Varying also the other parameters (for instance, we would not have to choose those $\tilde{J}$, $\tilde{K}$, etc. that yield a maximum possible value of ξ) we can fit both polarization and susceptibility.

The above discussion is, of course, futile, until a structural study can definitively identify the elements of the Rochelle salt structure that play the role of the ordering units. Implications of these findings could involve, along with the above mentioned simple change in the number of the ordering units per unit cell, more drastic changes to the model and, possibly, its extension to a four-sublattice one. Further experimental and theoretical studies of the Rochelle salt are thus requisite.

APPENDIX

The quantities $p_{\xi}^{\sigma_4}$ and $p_{\sigma}^{\sigma_4}$ entering the expression for specific heat [Eq. (2.24)] are

$$p_{\xi}^{\sigma_4}=\frac{\mu_1}{v}\left(\frac{\partial\xi}{\partial T}\right)_{\sigma_4}=p_{\xi}^{\varepsilon_4}+e_{\xi}\alpha_4,$$

$$p_{\sigma}^{\sigma_4}=\frac{\mu_1}{v}\left(\frac{\partial\sigma}{\partial T}\right)_{\sigma_4}=p_{\sigma}^{\varepsilon_4}+e_{\sigma}\alpha_4,$$

where

$$p_4=\left(\frac{\partial\sigma_4}{\partial T}\right)_{P_1,\varepsilon_4}=\frac{1}{T}q_4^{P_1},$$

$$p_{\xi}^{\varepsilon_4}=\frac{\mu_1}{v}\frac{1}{\Delta}\begin{vmatrix}N_1^T N_{12}\\ N_2^T N_{22}\end{vmatrix},\quad p_{\sigma}^{\varepsilon_4}=\frac{\mu_1}{v}\frac{1}{\Delta}\begin{vmatrix}N_{11}N_1^T\\ N_{21}N_2^T\end{vmatrix},$$

$$e_{\xi}=\frac{\mu_1}{v}\frac{1}{\Delta}\begin{vmatrix}N_1^{\varepsilon_4}N_{12}\\ N_2^{\varepsilon_4}N_{22}\end{vmatrix},\quad e_{\sigma}=\frac{\mu_1}{v}\frac{1}{\Delta}\begin{vmatrix}N_{11}N_1^{\varepsilon_4}\\ N_{21}N_2^{\varepsilon_4}\end{vmatrix},$$

$$N_1^T=-\frac{\gamma\rho-2\delta\xi\sigma}{2T},\quad N_2^T=-\frac{\delta\rho-2\gamma\xi\sigma}{2T};$$

$$N_{11}=1-\frac{\beta(J+K)}{4}\rho,\quad N_{12}=\frac{\beta(K-J)}{4}2\xi\sigma,$$

$$N_{21}=\frac{\beta(K+J)}{4}2\xi\sigma,\quad N_{22}=1+\frac{\beta(K-J)}{4}\rho,$$

$$N_1^{\varepsilon}=-\beta\psi_4\rho,\quad N_2^{\varepsilon}=-\beta\psi_4 2\xi\sigma,$$

$$\Delta=N_{11}N_{22}-N_{12}N_{21}.$$

[1] B. C. Frazer, M. McKeown, and R. Pepinsky, Phys. Rev. **94**, 1435 (1954).
[2] F.Jona and G. Shirane, *Ferroelectric Crystals* (Pergamon Press, Oxford, 1962).
[3] T. Mitsui, Phys. Rev. **111**, 1259 (1958).
[4] Y. Iwata, S. Mitani, and O. Shibuya, Ferroelectrics **96**, 215 (1989).
[5] Y. Iwata, S. Mitani, and O. Shibuya, Ferroelectrics **107**, 287 (1990).
[6] A. A. Volkov, Yu. G. Goncharov, G. V. Kozlov, Ye. B. Kryukova, and J. Petzelt, Pis'ma Zh. Éksp. Teor. Fiz. **41**, 16 (1985) [JETP Lett. **41**, 17 (1985)].
[7] A. A. Volkov, G. V. Kozlov, Ye. B. Kryukova, and A. A. Sobyanin, Fiz. Tverd. Tela (Leningrad) **28**, 797 (1986) [Sov. Phys. Solid State **28**, 444 (1986)].
[8] S. Kamba, G. Schaack, and J. Petzelt, Phys. Rev. B **51**, 14 998 (1995).
[9] J. Hlinka, J. Kulda, S. Kamba, and J. Petzelt, Phys. Rev. B **63**, 052102 (2001).
[10] E. Suzuki and Y. Shiozaki, Phys. Rev. B **53**, 5217 (1996).
[11] J. Kulda, J. Hlinka, S. Kamba, and J. Petzelt, ILL: Annual Report 2000. (www.ill.fr/AR-00/p-48.htm).
[12] V. G. Vaks, *Introduction into Microscopic Theory of Ferroelectrics* (Nauka, Moscow, 1973) (in Russian).
[13] B. Zeks, G. C. Shukla, and R. Blinc, Phys. Rev. B **3**, 2306 (1971).
[14] K. Mori, Ferroelectrics **31**, 173 (1981).
[15] J.Kalenik, Acta Phys. Pol. **48**, 387 (1975).
[16] B. Zeks, G. C. Shukla, and R. Blinc, J. Phys. Colloq., Suppl. 4, **33**, C2-C67 (1972).
[17] R. R. Levitskii, I. R. Zachek, and V. I. Varanitskii, Ukr. Phys. J. **25**, 1766 (1980) (in Russian).
[18] R. R. Levitskii, Yu. T. Antonyak, and I. R. Zachek, Ukr. Phys. J. **26**, 1835 (1981) (in Russian).
[19] R. R. Levitskii and R. O. Sokolovskii, Condens. Matter Phys. **2**, 393 (1999).
[20] F. Sandy and R. V. Jones, Phys. Rev. **168**, 481 (1968).
[21] J. Grigas *et al.*, Lithuanian Phys. Proc. **24**, 33 (1984) (in Russian).
[22] R. R. Levitskii, I. R. Zachek, and V. I. Varanitskii, Fiz. Tverd. Tela (Leningrad) **22**, 2750 (1980) [Sov. Phys. Solid State **22**, 1603 (1980)].
[23] V. A. Ambrazyavichene, A. A. Volkov, G. V. Kozlov, V. S. Krasikov, E. B. Kryukova, Fiz. Tverd. Tela (Leningrad) **25**, 1605 (1983) [Sov. Phys. Solid State **25**, 925 (1983)].
[24] R. R. Levitskii, T. M. Verkholyak, I. V. Kutny, and I. G. Hil, cond-mat/0106351 (unpublished).
[25] I. V. Stasyuk and I. N. Biletskii, Bull. Acad. Sci. USSR, Phys. Ser. (Engl. Transl.) **4**, 79 (1983).
[26] I. V. Stasyuk, R. R. Levitskii, I. R. Zachek, and A. P. Moina, Phys. Rev. B **62**, 6198 (2000).
[27] R. J. Glauber, J. Math. Phys. **4**, 294 (1963).
[28] I. V. Stasyuk and Yu. Dublenych (private communication).
[29] P. K. Dey, K. K. Som, K. R. Chowdhury, B. K. Sarkar, and B. K. Chaudhuri, Phys. Rev. B **47**, 3001 (1993).
[30] O. Yu. Serdobolskaya, Solid State Phys. **38**, 1529 (1996).
[31] J. Hablützel, Helv. Phys. Acta **12**, 489 (1939).
[32] H. Beige and A. Kühnel, Phys. Status Solidi A **84**, 433 (1984).
[33] W. J. Bronowska, J. Appl. Crystallogr. **14**, 203 (1981).
[34] W. G. Cady, *Piezoelectricity; An Introduction to the Theory and Application of Electromechanical Phenomena in Crystals* (McGraw Hill, New York, 1946).
[35] H. Mueller, Phys. Rev. **47**, 175 (1935).
[36] W. Taylor, D. J. Lockwood, and H. J. J. Labbe, J. Phys. C **17**, 3685 (1984).
[37] W. P. Mason, Phys. Rev. **55**, 775 (1939).
[38] V. M. Petrov, Sov. Phys. Crystallogr. **7**, 403 (1962).
[39] V. A. Yurin, Bull. Acad. Sci. USSR, Phys. Ser. (Engl. Transl.) **29**, 2001 (1965).
[40] W. P. Mason, Phys. Rev. **72**, 854 (1947).
[41] H. Akao and T. Sasaki, J. Chem. Phys. **23**, 2210 (1955).
[42] L. Gutin, Zh. Éksp. Teor. Fiz. **15**, 199 (1945).
[43] A. V. Shyl'nikov *et al.*, Kristallografiya **31**, 326 (1986) [Sov. Phys. Crystallogr. **31**, 192 (1986)].
[44] J. F. Araujo *et al.*, Phys. Rev. B **57**, 783 (1998).
[45] Y. M. Poplavko, V. V. Meriakri, P. Pereverzeva, and V. V. Alesheckin, and V. I. Molchanov, Fiz. Tverd. Tela (Leningrad) **15**, 2515 (1974) [Sov. Phys. Solid State **15**, 1672 (1974)].
[46] H. E. Müser and J. Pottharst, Phys. Status Solidi **109**, (1967).
[47] H. Kolodziej, in *Dielectric and Related Molecular Processes* (The Chemical Society Burlington House, London, 1975), Vol. 2, pp. 249–287.
[48] A. A. Volkov, G. V. Kozlov, and S. P. Lebedev, Zh. Éksp. Teor. Fiz. **79**, 1430 (1980) [Sov. Phys. JETP **52**, 722 (1980)].
[49] Yu. M. Poplavko and L. P. Solomonova, Bull. Acad. Sci. USSR, Phys. Ser. (Engl. Transl.) 1771 (1967).
[50] L. P. Pereverzeva, in *Mechanisms of Relaxation Phenomena in Solids* (Kaunas, 1974), p. 223 (in Russian).
[51] H. Deyda, Z. Naturforsch. A **22a**, 1139 (1967).
[52] W. Jäckle, Z. Angew. Phys. **12**, 148 (1960).
[53] D. Berlincourt, D. R. Currar, and H. Jaffe, see *Physical Acoustics* edited by P. W. Mason (Academic Press, New York, 1964), Vol. I, Pt. A, p. 162.
[54] W. J. Price, Phys. Rev. **75**, 946 (1949).
[55] I. M. Silvestrova, V. A. Yurin, L. A. Shuvalov, and A. V. Podlesskaya, Bull. Acad. Sci. USSR, Phys. Ser. (Engl. Transl.) **29**, 2005 (1965).
[56] R. Lichtenstein, Phys. Rev. **72**, 492 (1947).
[57] W. P. Mason, *Piezoelectric Constants and Their Application to Ultrasonics* (Van Nostrand, New York, 1950).
[58] A. R. Ubbelohde and I. Woodward, Proc. R. Soc., London, Ser. A **185**, 448 (1946).
[59] J. Helwig, Ferroelectrics **7**, 225 (1976).
[60] M. Tatsumi, T. Matsuo, H. Suga, and S. Seki, J. Phys. Chem. Solids **39**, 427 (1978).
[61] J. Helwig, Ferroelectrics **11**, 471 (1976).
[62] Y. M. Poplavko, N. V. Slesarenko, and L. A. Pasechnik, Fiz. Tverd Tela (Leningrad) **27**, 1248 (1985) [Sov. Phys. Solid State **27**, 755 (1985)].
[63] J. F. G. Hicks and J. G. Hooley, J. Am. Chem. Soc. **60**, 2994 (1938).
[64] G. G. Wiseman and J. K. Kuebler, Phys. Rev. **131**, 2023 (1963).
[65] K. Imai, J. Phys. Soc. Jpn. **39**, 868 (1975).
[66] R. Blinc and B. Žekš, Phys. Lett. A **39**, 167 (1972).